Clinical Biomechanics 130 (2025) 106671

Contents lists available at ScienceDirect

Clinical Biomechanics

journal homepage: www.elsevier.com/locate/clinbiomech

How does the collar in cementless hip stems work? Comparison of the strain distribution in the cortex of the proximal femur

Katja Brand [a,*], Golzar Dakhili [a], Frank Lampe [b,c], Benjamin Ondruschka [d], Michael M. Morlock [a], Gerd Huber [a]

[a] Institute of Biomechanics, TUHH Hamburg University of Technology, Hamburg, Germany
[b] Orthopedics and Trauma Surgery, Asklepios Klinik Barmbek, Hamburg, Germany
[c] Faculty of Life Sciences, Hamburg University of Applied Sciences, Hamburg, Germany
[d] Institute of Legal Medicine, University Medical Center Hamburg-Eppendorf, Hamburg, Germany

ARTICLE INFO

Keywords:
Cementless
Collar
Implantation process
Intraoperative periprosthetic fracture
Strain measurement
Total hip arthroplasty

ABSTRACT

Background: Collared cementless hip stems have demonstrated a reduced incidence of periprosthetic femoral fractures compared to collarless counterparts. Many fractures occur during implantation, when collarless stems are seated to achieve press-fit, causing critical tensile strains in the femur. Collared stems can limit excessive seating and subsidence through calcar-collar contact.
This study aimed to explain the clinically observed smaller fracture rates with collared stems by comparing strain distributions during implantation and loading between collared and collarless stems. It was hypothesized that collared stems distribute applied forces through both the collar and stem, increasing compressive axial and shear strains, allowing higher load tolerance.
Methods: Seven collared and seven collarless stems were implanted with constant velocity (0.1 mm/s) in porcine femurs until failure. Two human cadaveric femurs were tested as proof of concept. Shear, axial compressive and tangential tensile strains were compared alongside fracture patterns, subsidence and forces.
Findings: Collared stems in porcine femurs resisted approximately twice as much force until failure occurred (collared: 4187 N, collarless: 1980 N; $p < 0.001$), with similar tangential tensile strains (1 % to 1.4 % $p = 0.805$) and subsidence of 1.6 mm for collarless and 1.1 mm for collared stems at different failure forces ($p = 0.288$). Axial compressive strain was heavily increased by 1147 % with collared stems (collared: 1.2 %, collarless: 0.1 %; $p = 0.026$). Human femurs exhibited similar trends.
Interpretation: During loading, the collar prevents periprosthetic femoral fractures by increasing axial compressive strains instead of causing critical excessive tangential tensile strains (hoop strains) that can result in fractures.

1. Introduction

Periprosthetic femoral fractures (PFFs) are one of the main reasons for the revision of hip stems: In Germany, they dominantly cause 16 % of revisions (Grimberg et al., 2024) and are present in about 25 % of all revisions (Konow et al., 2021). In the American Joint Replacement Registry for the United States, 20 % of revisions during the early postoperative phase are linked to PFFs (Rosemont, 2024). Combining data from the National Joint Registry and the Hospital Episode Statistics in the UK exhibited that the total number of PFF cases is twice as high if cases treated with fixation are included since treatments with fixation are not covered in the joint registries (Lamb et al., 2024).

The majority of early PFFs are already caused intraoperatively (Capello et al., 2014). They initiate as small calcar cracks in the calcar region (Capello et al., 2014; Mont et al., 1992) and can be treated with cerclage wire to increase axial and rotational stability if directly detected (Fishkin et al., 1999; Park et al., 2020; Waligora et al., 2017). 60 % to 74 % of the calcar cracks are initiated during the preparation process with broaches while 16 % to 40 % during stem implantation followed by a small number of calcar cracks during other preparation steps (Abdel et al., 2016; Bellova et al., 2019; Fernandez-Fernandez et al., 2008; Mont et al., 1992).

* Corresponding author.
E-mail address: katja.glismann@tuhh.de (K. Brand).

https://doi.org/10.1016/j.clinbiomech.2025.106671
Received 3 March 2025; Accepted 15 September 2025
Available online 15 September 2025

However, up to 50 % of these small calcar cracks remain undetected during surgery (Schwartz Jr et al., 1989). When put under stress, these cracks can not only expand to PFFs, but also cause major stem migration requiring a revision (Gromov et al., 2017).

In several registry-based studies, collared cementless stems have been shown to decrease the PFF rate compared to their collarless counter parts (Konow et al., 2021; Lamb et al., 2019; Melbye et al., 2021). Especially for elderly female patients (> 80 years) the incidence of PFFs with cementless stems is 48 % lower when patients are treated with a collared instead of a collarless version (Morlock et al., 2024). This is noteworthy, since cemented stems are usually advised for this patient collective since they can also lower the risk by 46 % compared to collarless cementless stems (Morlock et al., 2024).

Good contact of the collar with the calcar (calcar-collar contact) is achieved by the calcar reamer used together with the last broach during surgery. The exposure of the reamed calcar also increases the visibility of calcar cracks in this region and can initiate cerclage wiring if needed to reduce PFF risk (Magill et al., 2016). Given a good calcar-collar contact collared stems were shown to withstand about 100 % higher forces before fracture compared to collarless stems when loaded vertically on the head of the prosthesis (Demey et al., 2011). They also increase the force needed for failure by 33 % when a horizontal fall on the hip is simulated (Demey et al., 2011) and the torsional load to failure is increased by up to 52 % (Johnson et al., 2020; Lamb et al., 2019).

So far the underlying failure mechanism of intraoperative PFFs is seen as excessive tangential tensile strains (hoop strains) caused by the intramedullary radial contact stress in the implant-bone interface (Mont et al., 1992; Park et al., 2020). Failure strains in a range of 0.24 % to 1 % have been reported to be crucial (Bayraktar et al., 2004; Elias et al., 2000; Jasty et al., 1993). Excessive subsidence is regarded as an indicator, but also as a potential cause of PFF since the subsiding stem can act as a riffing wedge in the femur (Aamodt et al., 2001; Elias et al., 2000; Herzwurm et al., 1992) (Bonnin et al., 2015). Collared stems are expected to reduce the risk of subsidence (Simpson et al., 2010; Syed et al., 2018), but whether other aspects in the strain distribution change like compressive strain has yet to be proven (Weightman et al., 1987).

The purpose of this study was therefore to explain the clinically observed reduction in PFF rates with collared stems by demonstrating the modified strain distribution of collared stems during the implantation and loading processes. The consequences of the calcar-collar contact will be analyzed for changes in the load situation.

It is hypothesized that collared stems will distribute applied forces via the collar and stem, thereby increasing axial compressive strain and shear strain, while keeping tangential tensile strain low. This will enable a higher force to be applied until a PFF occurs.

2. Methods

14 porcine femurs of slaughtered fattening pigs were stored below −20 °C for three months. Six exemplary femurs were CT-scanned (120 kV, 0.4 mm slice thickness, Incisive CT 128; Philips, Amsterdam, Netherlands) together with a calibration phantom (QSA; QRM, Mährendorf, Germany). A limited control group appeared to be reasonable since porcine femurs from the food chain were expected to be comparable (if not, being near to similar) in morphology and bone quality. Based on the phantom the CT Hounsfield units were transferred to bone mineral density (BMD) in terms of Calcium-hydroxy apatite content (Structural Insight 3; University Hospital Schleswig-Holstein, Kiel, Germany (Graeff et al., 2007)). A bone specific BMD parameter was determined by the mean value from a cubic region of interest (10 × 10 × 10 mm) at the center of the femoral head above the Ward's triangle (AVIZOLite 9.7.0; Thermo Fisher Scientific, Waltham, MA, US) (Glismann et al., 2024). Differences in Dorr types were identified based on the ratio between canal-to-calcar ratio (CCR) and cortical index (CI) (Dorr et al., 1988). The canal width was measured at the height of the isthmus which is 45 mm below the lesser trochanter for the porcine femurs. Comprehensive templating was not performed, since only one stem size was used for all porcine femurs.

After thawing to room temperature (Püschel et al., 2020), the distal end of the femurs were embedded with PMMA leaving 10 mm distance between the proximal surface of the embedment and the estimated position of the stem tip (Technovit 4004; Kulzer, Hanau, Germany) after implantation.

Preparation of the porcine cavities was performed by two biomechanical researchers that were familiar with stem implantation from human specimen studies. Broaching was performed with sharp extraction broaches followed by the corresponding compaction broaches on which the calcar reaming with a power tool was used (Corail, Johnson&Johnson MedTech, Warsaw, IN, US (DePuy Synthes, 2022a)).

The femurs were randomly assigned to two groups (each containing 3 CT-scanned and 4 un-scanned femurs, Fig. 1a). Implantations were performed depending on the group either with a collared or collarless fully porous hydroxyapatite-coated (HA) tapered stem designs (size 8, Corail, Johnson&Johnson MedTech; (DePuy Synthes, 2022a)). Apart from the collar the geometry of both stem designs is identical and the same surgical tools were used by the same surgeon.

In addition to the porcine femurs, two human cadaveric femurs were included to ascertain whether the behavior of the porcine femurs with thinner cortices might be transferred to the behavior of human femurs with thicker cortices.

The human cadaveric femurs were treated according to the porcine femurs. Femur morphology was also determined in the templating program (Velys Surgery), but the canal width was measured 100 mm below the lesser trochanter as defined by (Dorr et al., 1988). Preoperative templating (Velys Surgery) and implantation was performed on the human femurs by an experienced senior orthopedic surgeon with more than 1000 implantations using the established stem design (Fig. 1b).

Further differences were, that the distance between the expected stem tip position and the PMMA embedding was 70 mm; and that an electric power tool (Kincise, Johnson&Johnson MedTech) was used for broaching of the femur in accordance with the surgical technique (DePuy Synthes, 2022a; DePuy Synthes, 2022b). The greater trochanter was resected cranially by 10 mm to fit into the mechanical testing setup. Patient data were fully anonymized and no association between individual patient data and specimens were possible (see 2023–300,374-WF).

All femurs were hydrated with Ringer solution throughout the experiments. The stems were manually placed into the broached cavities. Implantation of the stems in porcine and human femurs was performed quasi-statically using a material testing machine (Z010; Zwick Roell; Fig. 2). The stem was continuously seated into the cavity with a speed of 0.1 mm/s. Although this method differs from the clinically applied hammer blows, it has produced equivalent results in terms of measuring strains (Elias et al., 2000). A moment free force application for the porcine femurs was achieved by using a polyethylene piston fixed to a floating bearing. A distal XY-table was solely used for alignment and locked during experimental loading (Fig. 2a). For the human femurs the force application was constrained and the XY-table was free to move (Fig. 2b).

Cortical strain was measured using digital image correlation in a target area extending from the reamed calcar to the lesser trochanter (digital image correlation - DIC, 15 Hz, 100 × 80 × 50 mm, ARAMIS 3D, MV 100; Carl Zeiss GOM Metropology GmbH, Oberkochen, Germany). The DIC system tracked the displacement of each point marker on the bone to determine the local strain changes. This target area was chosen because calcar cracks during implantation are expected to be initiated in this region (Park et al., 2020). The collar further is expected to engage with the cortical bone here (Aamodt et al., 2001; Elias et al., 2000; Levadnyi et al., 2021; Mansour et al., 1995). Additionally, previous studies observed differences between stem designs in this region (Enoksen et al., 2016; Freitag et al., 2021). When calcar-collar contact was visually achieved, the amount of applied force was recorded.

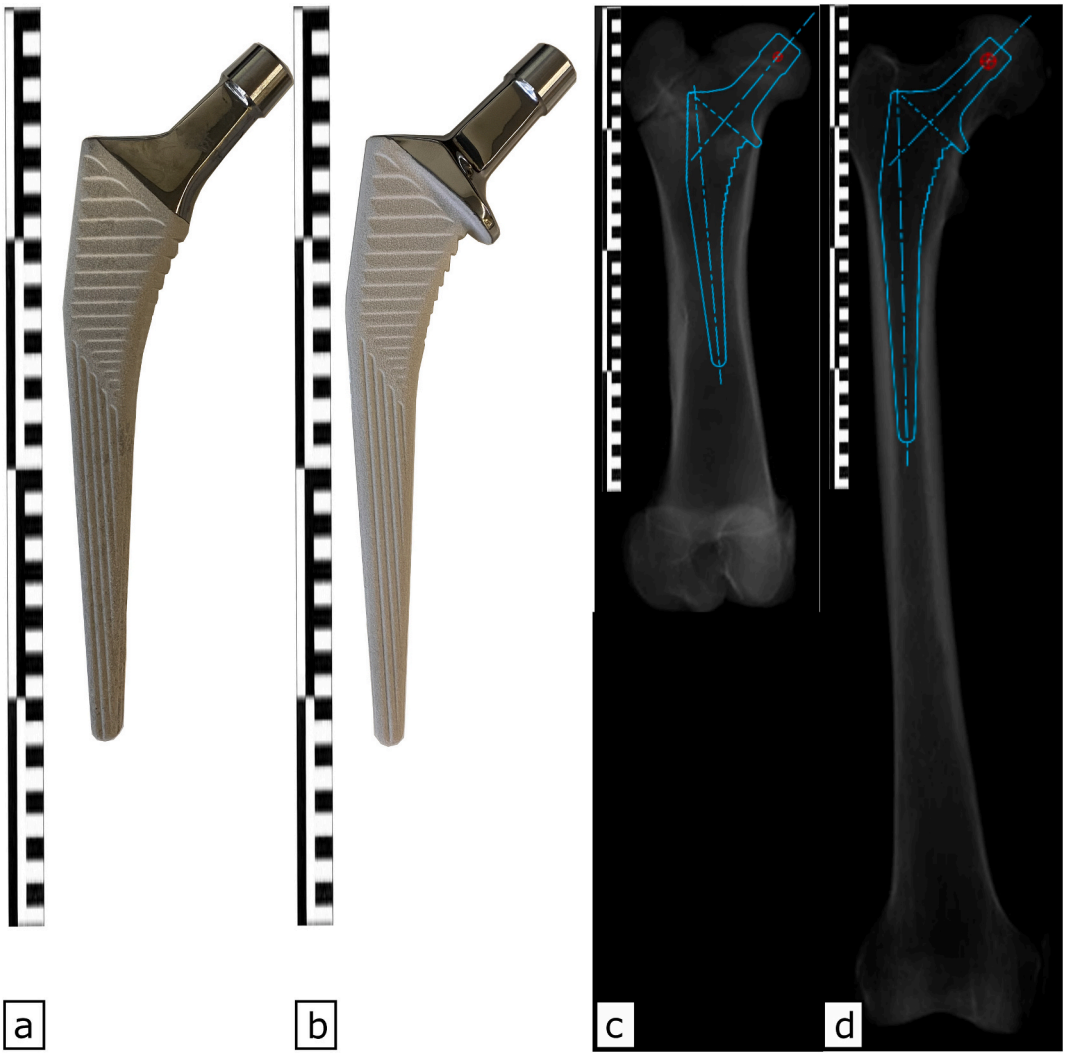

Fig. 1. (a) Corail stem size 12 (collarless version) and (b) Corail stem size 12 (collared version) with a larger scale compared to (c) templating of a porcine femur for a collared Corail size 8 and (d) templating of a human femur for a collared Corail size 11.

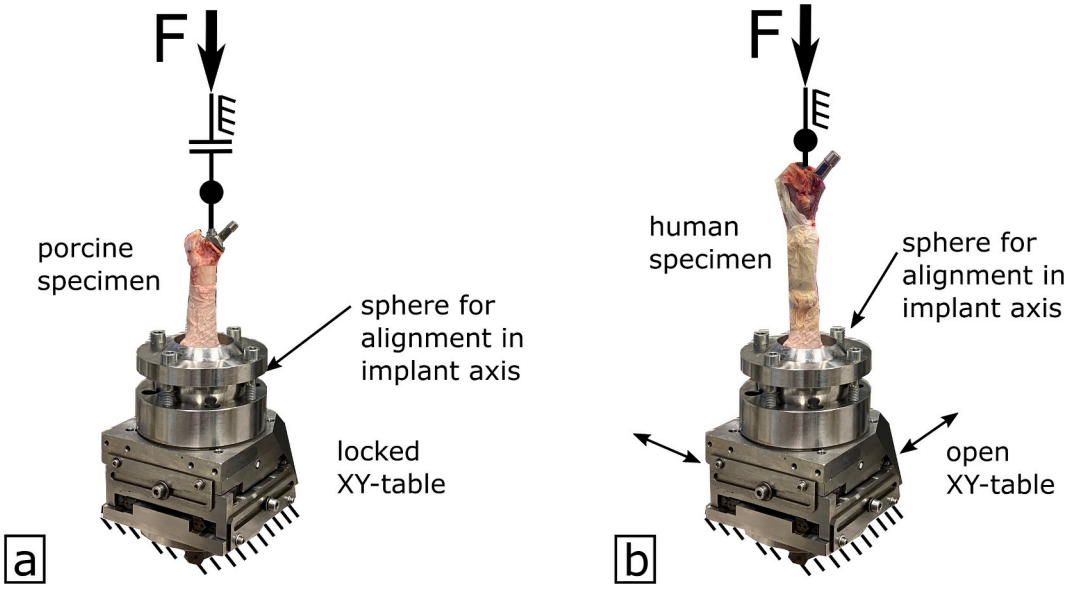

Fig. 2. The test set-up for quasi-static stem implantation. (a) For porcine femurs, the XY-table was locked and force was applied via a bearing that allowed horizontal movement while restricting the other degrees of freedom. (b) For human femurs, the XY-table was free to move and the force application was constrained to one axis.

Femurs were continuously visually inspected and three criteria for the termination of the load application were defined:

1) Visible periprosthetic fracture with acoustic crack sound
2) No visible periprosthetic fracture but excessive movement in setup - 40 mm movement of the test rig piston was exceeded for the porcine specimen or 40 mm translational movement of XY-table were exceeded for the human specimen, respectively
3) Force exceeds 5 kN or 8 kN for porcine or human femur, respectively.

The relative movement of the stem in relation to the femur was quantified by determining the distance between the markers attached to the stem and those on the femur. Therefore, local coordinate systems were established for both marker groups, and the Euclidean norm was computed to represent the overall magnitude of the relative motion (GOM Correlate 2018, Carl Zeiss GOM Metropology GmbH, Oberkochen, Germany, Fig. 3a). For collared stems calcar-collar contact was regarded as proper stem position for implantation (DePuy Synthes, 2022a). Due to similarity in the stem designs, the same seating depth for collarless implants was reached if the end of the coating was 1.2 mm superior of the resection plane. Subsequent axial stem movement was regarded as subsidence.

Mean technical strains (GOM Correlate 2018) in three directions similar to strain gauge rosettes were evaluated. Recorded data was filtered with a moving average over 5 values and the two principle strains with their phase were calculated (Matlab 2023, MathWorks, Natick, MA, US; Fig. 3b; (Hoffmann, 1987)). Based on this the I) tangential tensile strains (positive), the II) axial compressive strains along the implant axis (negative) and III) the corresponding shear strain were evaluated (Elias et al., 2000; Freitag et al., 2021).

Given that the geometry of the femur is not circular, the term "tangential strains" will be employed instead of circumferential strains or hoop strains used in some literature (Aamodt et al., 2001; Decking et al., 2006; Elias et al., 2000; Reilly and Burstein, 1975).

The highest and lowest values for strains before fracture were analyzed and are referred to as peak values. The applied force on porcine femurs was split into intervals of 100 N in which the maximum tangential tensile strain for each specimen and both stem designs was calculated. In each interval the mean and standard deviation were subsequently calculated for each stem design.

Statistical analyses were exclusively performed on the porcine specimens with a type I error level of 0.05 for all tests (SPSS 26.0, SPSS Inc., Chicago, NY, US). Data was checked for normality and homogeneity of variance. Parametric distributed data was analyzed using unpaired *t*-tests and displayed with bar charts (mean ± standard deviation), while non-parametric data was analyzed using Mann-Whitney-*U* Tests (MWU) and presented by box plots (median with interquartile range). Samples more than 1.5 points outside the interquartile ranges (outliers) were kept in all analyses after checking for measurement errors. Type I error probabilities between 0.05 and 0.10 are denoted as trends. No statistical tests were performed on the results from the CT scans due to the small sample size.

3. Results

Porcine femurs exhibited a thin cortex in all CT-scans leading to a similar canal to calcar ratio as in femurs of Dorr type C in five of six cases. One femur was thinner, leading to a morphology similar to a Dorr type A. The porcine femurs exhibited a higher BMD than the human femurs of donors aged 80 and 85. Specific data on sex, age and height for the porcine animals, however, was not available. Results are further specified in Table 1.

3.1. Fracture patterns vary between stem designs

Collarless stems caused higher tangential tensile strains on the cortex (red in Fig. 4a compared to 4d). All of these femurs developed calcar cracks (Fig. 4c). Femurs with collared stems showed pronounced axial compressive strain directly underneath the collar (blue in Fig. 4e compared to Fig. 4b) and exhibited different fracture patterns: one femur showed a calcar crack, two exhibited cortical bone that was displaced medially and detached from the trabecular bone, three showed compression of the cortical bone underneath the collar (Fig. 4f) and one femur did not fracture after being exposed to 5 kN.

3.2. Similarities and differences in strains, fracture forces and subsidence

The interrelation between the applied forces and the increase of the mean tangential tensile strain differed between femurs with collarless and collared stems (Fig. 5). The collarless femurs caused an early increase with an intermediate drop caused by the statistical effect of an early failure to a maximum at 2.5 kN when all collarless femurs had failed. Tangential tensile strain in femurs with collared stems was also increased, but clearly stayed below the last peak of the collarless stems even for applied forces up to 5 kN.

Failure forces for femurs with collarless stems were always lower than those for femurs with collared stems (52.7 %; collarless: 1979.8 ± 406.3 N; collared 4187.1 ± 639.5 N; $p < 0.001$; independent-samples *t*-test; Figs. 5 and 8a), but despite that severe difference in fracture forces, the maximum tangential tensile strains until fracture were similar for both designs (collarless: 1.00 % [0.51 %, 2.07 %]; collared: 1.37 % [0.62 %, 2.90 %]; $p = 0.805$, Wilcoxon test; Fig. 7a). However, the peak axial compressive strain was increased by 1147 % for the collared stems (collarless: 0.096 % [0.036 %, 0.283 %]; collared: 1.197 % [0.305 %,

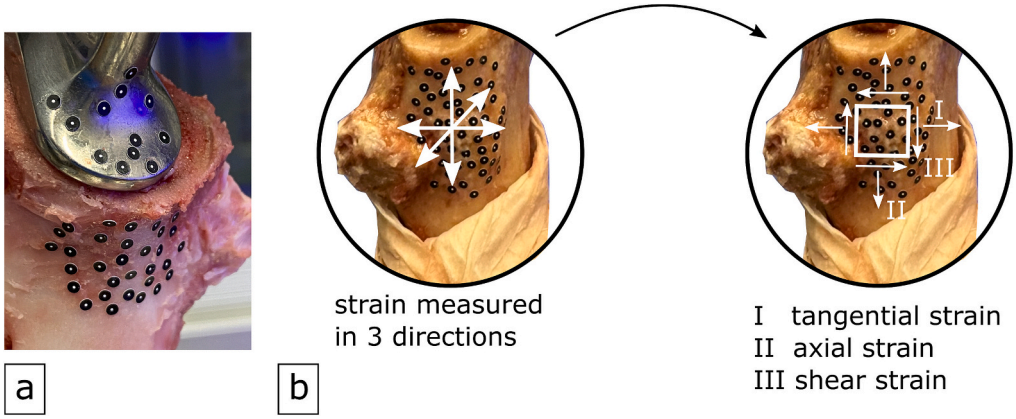

Fig. 3. (a) Point markers on the femur and the stem. (b) Strains along three axes were evaluated directly from the DIC measurement and transformed to the tangential and axial compressive strains, as well as the corresponding shear strain.

Table 1
Characteristics of the CT-scanned human and porcine femurs.

	Stem design	Sex	Age [years]	Height [mm]	Weight [kg]	BMD [mgHA/cm^3]	CCR/CI	Dorr
Porcine	Collarless					373.8	1.89	C
	Collarless					439.8	0.99	A
	Collared					421.3	2.08	C
	Collared					370.5	1.64	C
	Collarless					385.6	1.92	C
	Collared					468.9	1.60	C
Human	Collarless	F	80	1600	48.9	219.6	1.73	C
	Collared	F	85	1520	50.0	284.4	1.68	C

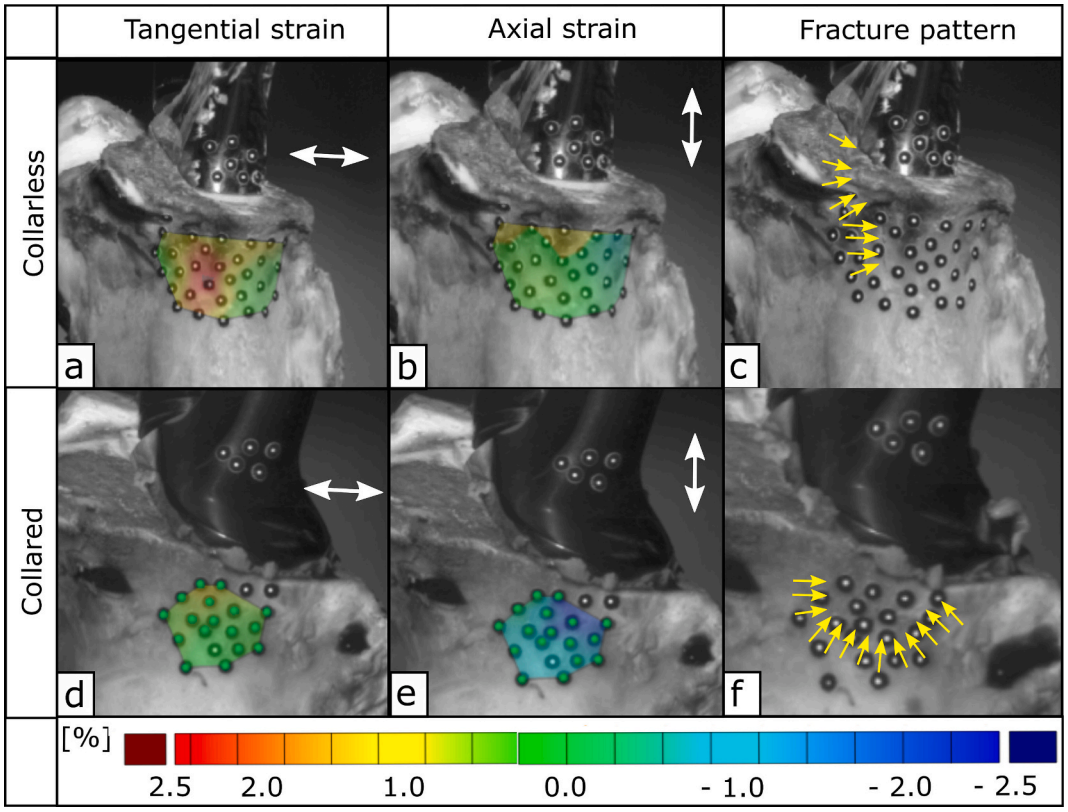

Fig. 4. Strain distribution (in percentage, directions indicated with white arrows) and resulting fracture pattern (indicated in yellow) in porcine femurs (top row collarless, bottom row collared stem). (For interpretation of the references to colour in this figure legend, the reader is referred to the web version of this article.)

2.093 %]; $p = 0.026$, Wilcoxon test; Figs. 6 and 7b).

Peak shear strain showed a tendency to be higher for the collared stems (collarless: 0.165 % [− 0.874 %, 0.519 %]; collared: 1.072 % [0.223 %, 1.241 %]; $p = 0.097$, Wilcoxon test; Fig. 7c).

The subsidence for collarless stems was 48 % higher at lower failure forces, however, this difference was not found to be statistically significant (collarless: 1.63 ± 1.14 mm; collared: 1.10 ± 0.54 mm; $p = 0.288$, independent-samples t-test; Fig. 8b). The collarless stem showing no subsidence fractured before the optimal position was reached.

3.3. Including human specimens

Both human femurs showed calcar cracks that run from the medial calcar distally (Fig. 9).

The human femurs exhibited almost half the fracture force with collarless compared to the collared implants. Compared to the porcine specimens a 63 % and 75 % higher fracture force was reached, respectively (collarless: 3465.0 N; collared: 6823.8 N; Fig. 8a). Furthermore, higher subsidence for collarless than collared stems was observed with a 218 % and 184 % rise, respectively (collarless: 5.18 mm; collared: 3.21 mm; Fig. 8b).

In the human femur the highest tangential tensile strain before fracture for the collarless stem was in the upper region as it was seen for porcine femurs (collarless: 2.51 %) while for the collared stem hardly any tangential tensile strain was observed (collared: 0.01 %; Fig. 7a). The axial compressive strains in the human femurs were within the interquartile range of the results for the porcine femurs and the collared stem showed higher peak axial compressive strain compared to the collarless stem (collarless: 0.0582 %, collared: 0.461 %, Fig. 7b). The shear strains in the human femurs were slightly outside the whiskers of the porcine measurements (collarless: 1.075 %, collared: −0.0441 %, Fig. 7c).

4. Discussion

During quasi-static implantation of collarless and collared stems, differences in strain on the cortex of the femora might explain the clinically observed smaller PFF rates with collared stems.

In-vitro implantation by a quasi-static continuously increasing load application instead of a clinic-like dynamic force application via a mallet

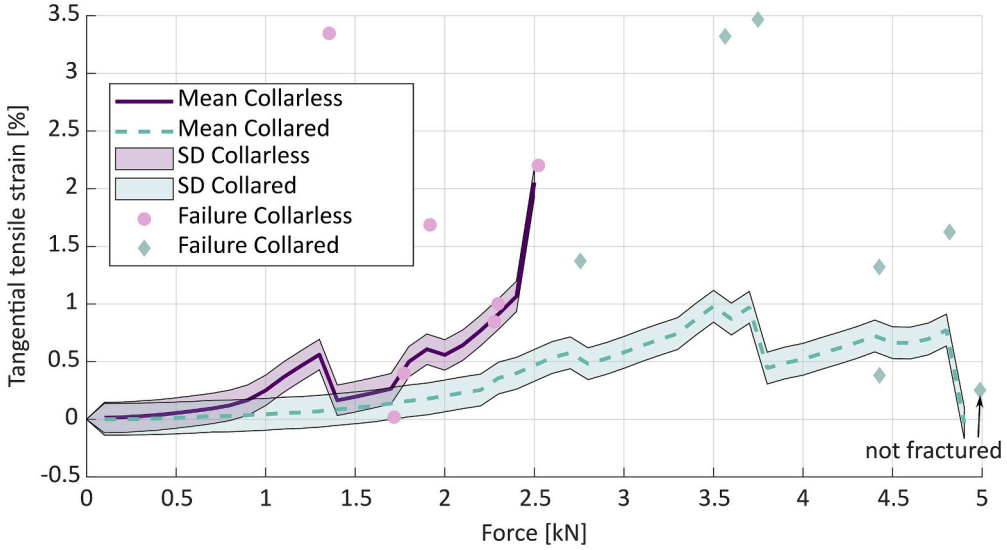

Fig. 5. Collarless stems reach mean tangential tensile strains leading to PFFs already at lower forces compared to collared stems. Sudden changes in the mean tangential tensile strain can be explained by the number of specimens decreasing through PFFs at higher forces. (SD, standard deviation).

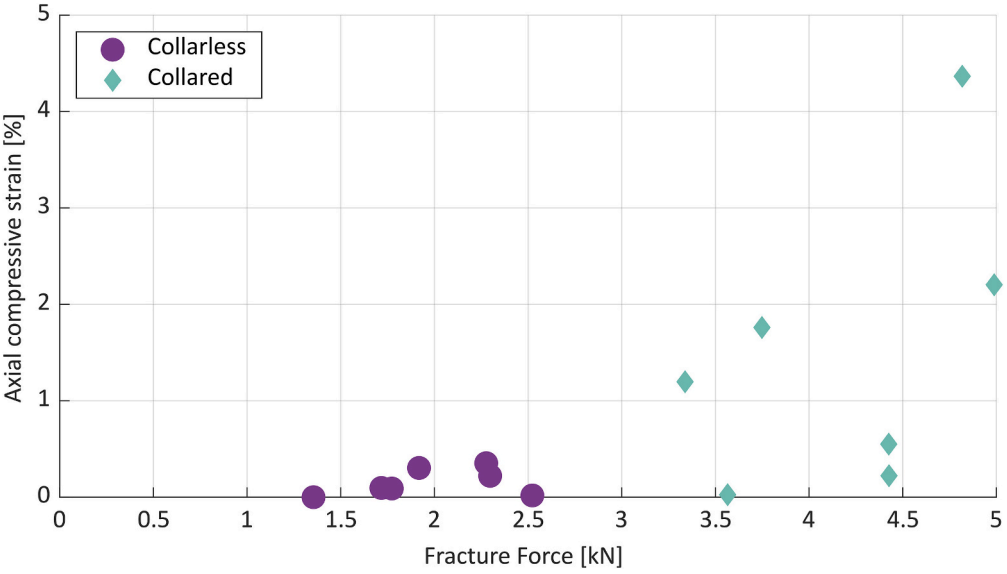

Fig. 6. Collarless stems exhibited less peak axial compressive strains compared to collared stems, which can be loaded with higher forces.

is an established method, since similar strain distributions propagating on the medial cortical femur were found - regardless of the load application (Elias et al., 2000).

The dynamic mallet impaction in the clinical setting may be a relevant source for PFFs. Attempts were made to control it by the use of automated impactors (Konow et al., 2022). In this study replacing the dynamic impaction by a controlled quasi-static continuous implantation appears to be justified, since all collarless stems failed due to calcar cracks alike those observed for intraoperative PFFs (Elias et al., 2000; Jakubowitz et al., 2009; Varga et al., 2016; Wendler et al., 2022). For collared stems, one femur showed a calcar crack, five of seven porcine femurs experienced compression fracture patterns which are not yet described in clinics and one porcine femur did not fracture after being exposed to 5kN max.

DIC measurements allowed the capture of a more extensive target area than seen in previous studies with strain gauges (Aamodt et al., 2001; Elias et al., 2000; Freitag et al., 2021; Huber and Technische Universität Hamburg-Harburg, 2005; Jasty et al., 1993; Rudman et al., 2006), capturing the fracture region in 12 of 13 porcine samples. The accuracy of the DIC is lower compared to strain gauges (International Digital Image Correlation Society, 2018), but the fracture behavior of the femurs, were less affected by point markers for DIC than strain gauges, since no surface processing including degreasing was required and no alteration of the mechanical properties of the femur, by the layers of glue and the strain gauges carrier foil was needed. The representation of the strain in an anatomically based coordinate system – consisting of tangential, axial and shear components - was employed instead of the representation with principle strains (Elias et al., 2000), since this choice directly illustrates the collar's influence during quasi-static implantation.

Porcine femurs are commonly used as models due to their availability in homogenous groups with regard to age, size, weight and health status. However, the CT-data exhibited higher variability in Dorr type as well as BMD than expected. Further studies should therefore include this information to ensure homogenous groups. CT-data was included in this study to enable a comparison between the porcine and human femurs

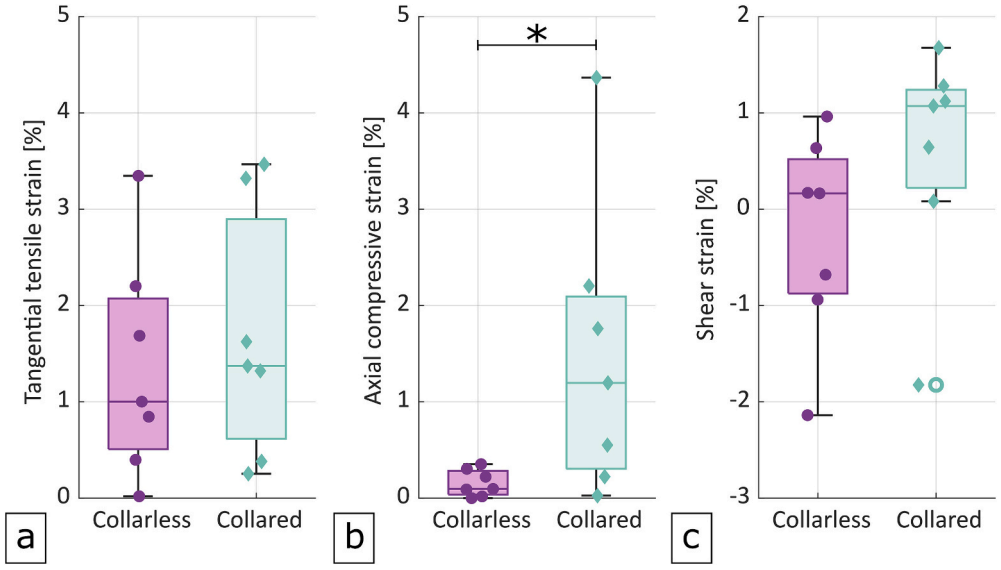

Fig. 7. The three strain components at the antero-medial cortex prior periprosthetic fracture with lower failure forces for collarless and higher ones for collared stems: (a) tangential tensile strain and (b) axial compressive strain, the star (*) indicates $p < 0.05$. (c) Shear strains with an outlier (circle) of >1.5*IQR.

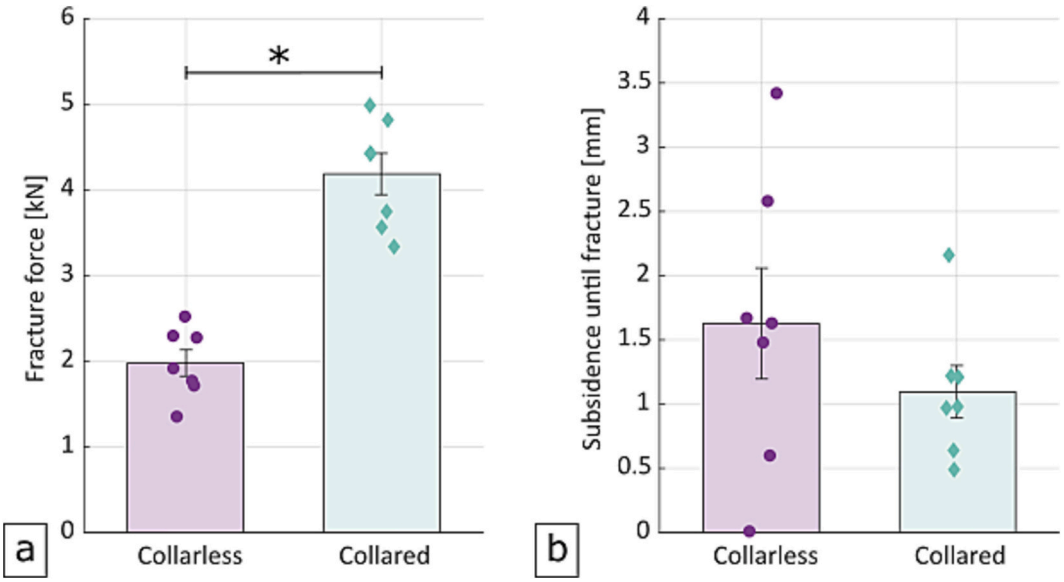

Fig. 8. (a) Fracture forces and (b) subsidence for the collarless and collared stems of the porcine specimens (the star (*) indicates $p < 0.05$).

and to exclude severe anatomical abnormalities.

Porcine femurs possess high BMD due to their age of typically six months (Bundesinformationszentrum Landwirtschaft (BZL) Redaktion, 2022) and require the use of the smallest commercially available stem size due to their length. However, the canal-to-calcar ratio and cortical index as well as the corresponding Dorr type of porcine femurs with their thin cortex and wide canal, resembling human femurs of Dorr type C. These parameters are alike those of elderly women (Dorr et al., 1988; Konow et al., 2022), who are often affected by intraoperative fractures and benefit from cementless collared stems (Morlock et al., 2024).

Similar to a previous biomechanical study (Demey et al., 2011) significantly higher forces could be applied to porcine femurs implanted with collared stems compared to ones implanted with collarless stems. The forces to failure were in the range previously reported for human femurs during quasi-static implantation (1900 to 9550 N (Elias et al., 2000)), but were located in the lower range since porcine femurs have thinner cortices and their smaller diameter causes more radial pressure to be induced through similar axial force.

The measured tangential tensile strains are higher than previously published results from strain gauges on human femurs (0.24 % to 1 % (Bayraktar et al., 2004; Elias et al., 2000; Jasty et al., 1993)), probably because of the high local resolution and the wide measurement range of the DIC not missing peak values. Despite differences in failure forces, the tangential tensile strains at bony failure of both designs were similar, so that these tangential tensile strains might be regarded as cause for the introduction of PFFs (Elias et al., 2000). The shear strains are also higher than previously reported values on the medial tibia, but in literature they were measured in vivo and not related to PFFs (Al Nazer et al., 2012; Milgrom et al., 2000).

The axial compressive strain in porcine femurs was nine times higher for collared stems compared to the respective published values on human femurs (0.132 % (Elias et al., 2000; Jasty et al., 1993)). For collarless stems it was 27 % lower. They had in common that the axial compressive strain was higher in collared stems compared to collarless

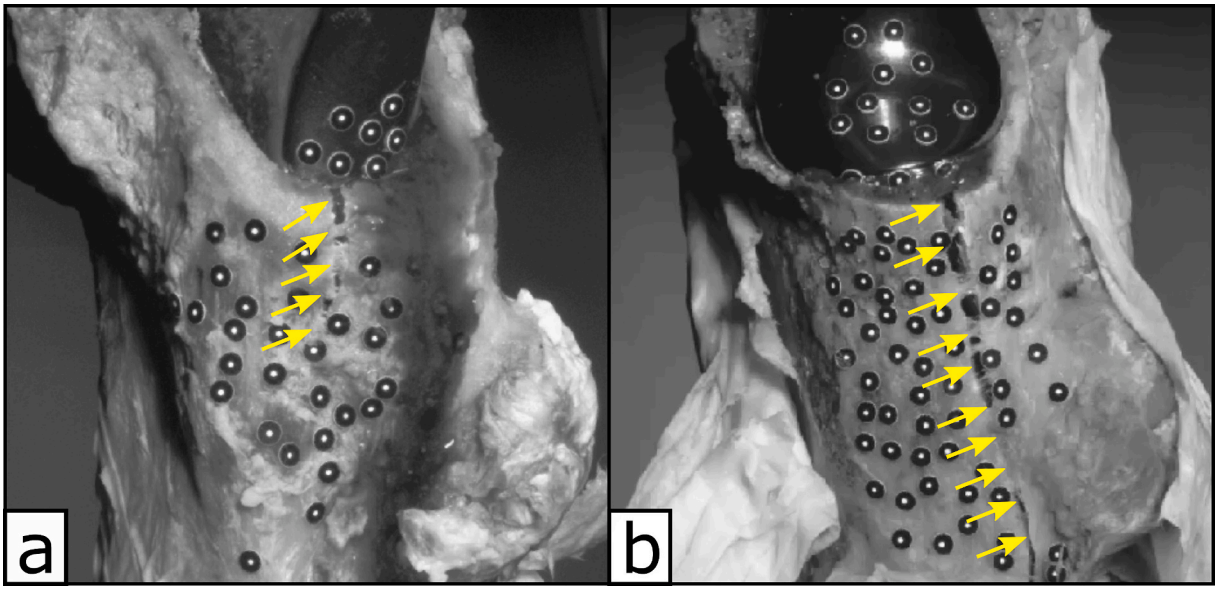

Fig. 9. The two human femurs implanted with (a) a collarless and (b) a collared stem showed similar periprosthetic fracture patterns (yellow). (For interpretation of the references to colour in this figure legend, the reader is referred to the web version of this article.)

stems. This indicates load sharing within the cortical bone of the calcar region, while a reduced part of the load is transmitted through the wedged stem (difference in radial and axial forces, Fig. 10, (Aamodt et al., 2001; Decking et al., 2006)). Consequently, radial pressure through the wedged stem is smaller leading to less tangential tensile strain (difference in radial forces, Fig. 10). Therefore, PFFs are reached at higher forces for collared stems than for collarless implants (Fig. 10).

The subsidence does not yield significant differences between stem designs. A power analysis determined that a sample size of 39 in each group would be required to exhibit a potential difference between the designs. The negligible difference in subsidence can be interpreted as similar high primary stability for both designs (Kistler et al., 2024). The recorded subsidence for porcine femurs was mostly lower than that reported for human femurs (Al-Najjim et al., 2016; Meding et al., 1997), probably due to the higher BMD of the porcine bones. It needs to be highlighted that ahead of failure, collarless stems subsided the same depth as collared stems but at significantly lower forces.

Three samples behaved differently: One femur of the collarless group exhibited almost no tangential tensile strain which might be connected to technical errors with the setup so that the fracture appeared aside the observed target area. Two of the collared stems did not show a pronounced axial compressive strain during loading. It is likely that no contact between collar and calcar was achieved, but no additional information is available on that. The results of these three samples remain included in this analysis since they did not change the general outcome.

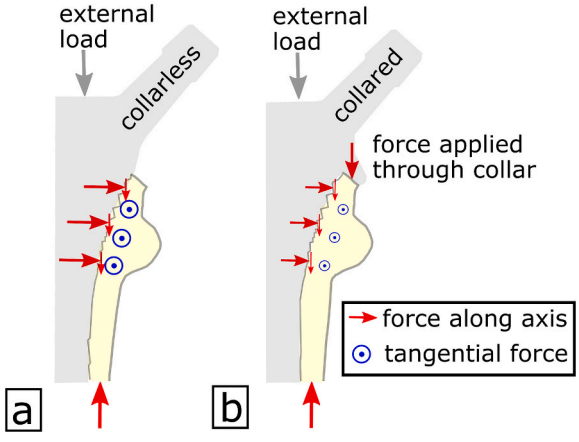

Fig. 10. Load distribution in (a) a collarless and (b) a collared stem.

The exemplary human femurs for collarless and collared stems showed an increased force for the collared stem with a higher axial compressive strain. For the collarless stem the tangential tensile strain was similar to the porcine specimens. However, the collared stem does not show an increase in tangential tensile strain even though the fracture pattern is a calcar crack. This phenomenon can be attributed to the fact that the target area is larger in the longer human femurs, which on average leads to lower strains near the fracture region. Overall, the human femurs showed parallels to the results for the porcine femurs, suggesting similar failure mechanisms.

One further limitation is the use of in-vitro experiments, neglecting soft tissues. No CT-scans were obtained post cavity preparation, which prevented the analysis of variations in the prepared cavity between specimens and the lack of information regarding the contact situation of the collar.

This study focused on the intraoperative situation of one specific stem design, thus it is unclear whether the observed load sharing can be generalized to the long-term situations as well as other designs.

Templating and proper sizing is demanding for collared stems to achieve a sufficient press-fit and enable subsequent bony ingrowth (Magill et al., 2016). Oversizing could make the collar useless while undersizing must be prevented since it can result in micromotions and even loosening (Kistler et al., 2024; McConnell et al., 2021). However, collared stems show a superior behavior towards applied forces compared to cementless collarless stems and registry-data exhibited, that they can perform similar to cemented stems in elderly women (Morlock et al., 2024).

5. Conclusion

In quasi-static implantation for equivalent forces, femurs with calcar-collar contact exhibited lower tangential tensile strains in comparison to femurs without. At failure the tangential tensile strain is similar, but the axial strain significantly increased for collared stems. It is concluded that delaying critical tangential tensile strains by increasing shear and axial compressive strains is the mechanism that improves the mechanical performance of collared stems.

CRediT authorship contribution statement

Katja Brand: Writing – original draft, Visualization, Validation, Software, Resources, Methodology, Investigation, Formal analysis, Data curation, Conceptualization. **Golzar Dakhili:** Writing – review & editing, Investigation, Formal analysis, Data curation. **Frank Lampe:** Writing – review & editing, Data curation. **Benjamin Ondruschka:** Writing – review & editing, Resources, Project administration. **Michael M. Morlock:** Writing – review & editing, Supervision, Project administration, Funding acquisition. **Gerd Huber:** Writing – review & editing, Supervision, Methodology, Funding acquisition, Conceptualization.

Declaration of competing interest

MMM reports financial support was provided by Johnson & Johnson MedTech. FL reports a relationship with Johnson & Johnson MedTech that includes: consulting or advisory. FL reports a relationship with Aesculap AG that includes: consulting or advisory. MMM reports a relationship with Johnson & Johnson MedTech that includes: consulting or advisory, funding grants, and speaking and lecture fees. MMM reports a relationship with CeramTec GmbH that includes: funding grants and speaking and lecture fees. MMM reports a relationship with Peter Brehm GmbH that includes: funding grants. MMM reports a relationship with Mathys Enovis that includes: speaking and lecture fees. BO is member of the board of the German Society of Legal Medicine; GH is member of the board of the German Society of Biomechanics.

Acknowledgements

The authors gratefully acknowledge the financial support of Johnson & Johnson MedTech. Johnson & Johnson MedTech was not involved in data evaluation or writing of the manuscript.

References

Aamodt, A., Lund-Larsen, J., Eine, J., Andersen, E., Benum, P., Husby, O.S., Aug. 2001. Changes in proximal femoral strain after insertion of uncemented standard and customised femoral stems: an experimental study in human femora. J. Bone Joint Surg. (Br.) 83-B (6), 921–929. https://doi.org/10.1302/0301-620X.83B6.0830921.

Abdel, M.P., Watts, C.D., Houdek, M.T., Lewallen, D.G., Berry, D.J., Apr. 2016. Epidemiology of periprosthetic fracture of the femur in 32 644 primary total hip arthroplasties: a 40-year experience. Bone Joint J. 98-B (4), 461–467. https://doi.org/10.1302/0301-620X.98B4.37201.

Al Nazer, R., Lanovaz, J., Kawalilak, C., Johnston, J.D., Kontulainen, S., Jan. 2012. Direct in vivo strain measurements in human bone—a systematic literature review. J. Biomech. 45 (1), 27–40. https://doi.org/10.1016/j.jbiomech.2011.08.004.

Al-Najjim, M., Khattak, U., Sim, J., Chambers, I., Dec. 2016. Differences in subsidence rate between alternative designs of a commonly used uncemented femoral stem. J. Orthop. 13 (4), 322–326. https://doi.org/10.1016/j.jor.2016.06.026.

Bayraktar, H.H., Morgan, E.F., Niebur, G.L., Morris, G.E., Wong, E.K., Keaveny, T.M., Jan. 2004. Comparison of the elastic and yield properties of human femoral trabecular and cortical bone tissue. J. Biomech. 37 (1), 27–35. https://doi.org/10.1016/S0021-9290(03)00257-4.

Bellova, P., Baecker, H., Lotzien, S., Brandt, M., Schildhauer, T.A., Gessmann, J., Dec. 2019. Risk analysis and clinical outcomes of intraoperative periprosthetic fractures: a retrospective study of 481 bipolar hemiarthroplasties. J. Orthop. Surg. 14 (1), 432. https://doi.org/10.1186/s13018-019-1494-1.

Bonnin, M.P., Neto, C.C., Aitsiselmi, T., Murphy, C.G., Bossard, N., Roche, S., Jun. 2015. Increased incidence of femoral fractures in small femurs and women undergoing uncemented total hip arthroplasty – why? Bone Joint J. 97-B (6), 741–748. https://doi.org/10.1302/0301-620X.97B6.35022.

Bundesinformationszentrum Landwirtschaft (BZL) Redaktion, Apr. 2022. Schweinemast in Deutschland – Ein Überblick. Accessed: Dec. 03, 2024. [Online]. Available: https://www.nutztierhaltung.de/schwein/mast/.

Capello, W.N., D'Antonio, J.A., Naughton, M., Feb. 2014. Periprosthetic fractures around a cementless hydroxyapatite-coated implant: a new fracture pattern is described. Clin. Orthop. Relat. Res. 472 (2), 604–610. https://doi.org/10.1007/s11999-013-3137-x.

Decking, R., Puhl, W., Simon, U., Claes, L.E., Jun. 2006. Changes in strain distribution of loaded proximal femora caused by different types of cementless femoral stems. Clin. Biomech. 21 (5), 495–501. https://doi.org/10.1016/j.clinbiomech.2005.12.011.

Demey, G., Fary, C., Lustig, S., Neyret, P., Selmi, T.A. Si, Dec. 2011. Does a collar improve the immediate stability of uncemented femoral hip stems in total hip arthroplasty? A bilateral comparative cadaver study. J. Arthroplast. 26 (8), 1549–1555. https://doi.org/10.1016/j.arth.2011.03.030.

DePuy Synthes, 2022a. Surgical Technique CORAIL Total Hip System. Accessed: Jan. 02, 2023. [Online]. Available: https://p1.aprimocdn.net/jjamp/en/depuy-synthes/ous-only-%E2%80%93-surgical-technique-guide-(stg)/198918-170655.pdf. Accessed: Sep. 16, 2025.

DePuy Synthes, 2022b. Kincise™ Application of Energy in Total Hip Arthroplasty. Accessed: Apr. 02, 2024. [Online]. Available: https://jnjinstitute.com/sites/default/files/2018-10/093648-180710%20KINCISE%20Surgical%20Automated%20System_Energy%20Analysis_DPS%20FINAL.pdf.

Dorr, L.D., Mackel, A.M., Malluche, H.H., Claude-Aaugere, M., 1988. Classification of femoral bone type for total hip arthroplasty. In: Presented at the Proceedings of the 55th Annual Meeting of American Academy of Orthopaedic Surgeons, Atlanta.

Elias, J.J., Nagao, M., Chu, Y.-H., Carbone, J.J., Lennox, D.W., Chao, E.Y.S., Jan. 2000. Medial cortex strain distribution during noncemented total hip arthroplasty. Clin. Orthop. 370, 250–258. https://doi.org/10.1097/00003086-200001000-00025.

Enoksen, C.H., Gjerdet, N.R., Klaksvik, J., Arthursson, A.J., Schnell-Husby, O., Wik, T.S., Feb. 2016. Deformation pattern and load transfer of an uncemented femoral stem with modular necks. An experimental study in human cadaver femurs. Clin. Biomech. 32, 28–33. https://doi.org/10.1016/j.clinbiomech.2016.01.001.

Fernandez-Fernandez, R., García-Elias, E., Gil-Garay, E., Jun. 2008. Peroperative fractures in uncemented total hip arthrography: results with a single design of stem implant. Int. Orthop. 32 (3), 307–313. https://doi.org/10.1007/s00264-006-0318-1.

Fishkin, Z., Han, S.-M., Ziv, I., Jan. 1999. Cerclage wiring technique after proximal femoral fracture in total hip arthroplasty. J. Arthroplast. 14 (1), 98–101. https://doi.org/10.1016/S0883-5403(99)90209-7.

Freitag, T., Bieger, R., Kiefer, H., Dornacher, D., Reichel, H., Ignatius, A., Dürselen, L., Dec. 2021. Biomechanics of a calcar loading and a shortened tapered femoral stem: comparative in-vitro testing of primary stability and strain distribution. J. Exp. Orthop. 8 (1), 74. https://doi.org/10.1186/s40634-021-00388-1.

Glismann, K., Konow, T., Lampe, F., Ondruschka, B., Huber, G., Morlock, M.M., Apr. 2024. Small design modifications can improve the primary stability of a fully coated tapered wedge hip stem. PLoS One 19 (4), e0300956. https://doi.org/10.1371/journal.pone.0300956.

Graeff, C., Timm, W., Nickelsen, T.N., Farrerons, J., Marín, F., Barker, C., Glüer, C.C., Jun. 2007. Monitoring teriparatide-associated changes in vertebral microstructure by high-resolution CT in vivo: results from the EUROFORS study. J. Bone Miner. Res. 22 (9), 1426–1433. https://doi.org/10.1359/jbmr.070603.

Grimberg, A., Kirschner, S., Lützner, J., Melsheimer, O., Morlock, M., Steinbrück, A., 2024. EPRD Jahresbericht 2024. EPRD Endoprothesenregister Deutschland, DE Accessed: Sep. 16, 2025. [Online]. Available: doi: 10.36186/reporteprd102024.

Gromov, K., Bersang, A., Nielsen, C.S., Kallemose, T., Husted, H., Troelsen, A., Apr. 2017. Risk factors for post-operative periprosthetic fractures following primary total hip arthroplasty with a proximally coated double-tapered cementless femoral component. Bone Joint J. 99-B (4), 451–457. https://doi.org/10.1302/0301-620X.99B4.BJJ-2016-0266.R2.

Herzwurm, P.J., Walsh, J., Pettine, K.A., Ebert, F.R., Feb. 1992. Prophylactic cerclage: a method of preventing femur fracture in uncemented total hip arthroplasty. Orthopedics 15 (2), 143–146. https://doi.org/10.3928/0147-7447-19920201-06.

Hoffmann, K., 1987. Eine Einführung in die Technik des Messens mit Dehnungsmessstreifen. Hottinger Baldwin Messtechnik, Darmstadt.

Verhalten von Wirbelsäulensegmenten bei dynamischer Belastung: Abschlussbericht zum Projekt "Experimentelle in-vitro Bestimmung der Belastbarkeit von Segmenten der Lendenwirbelsäule bei wiederholten praxisrelevanten (Ganzkörperschwingungen) Belastungen durch Kompressions- und Schubkräfte" - Projekt F 1899. In: Huber, G., Technische Universität Hamburg-Harburg (Eds.), 2005. Schriftenreihe der Bundesanstalt für Arbeitsschutz und Arbeitsmedizin Forschung, 1062. Wirtschaftsverl. NW, Verl. für Neue Wiss, Bremerhaven.

International Digital Image Correlation Society, 2018. A Good Practices Guide for Digital Image Correlation - Standardization, Good Practice, and Uncertainty Quantification. Accessed: Dec. 21, 2024. [Online]. Available: https://idics.org/guide/DICGoodPracticesGuide_PrintVersion-V5h-181024.pdf.

Jakubowitz, E., Seeger, J.B., Kretzer, J.P., Heisel, C., Kleinhans, J.A., Thomsen, M., Nov. 2009. The influence of age, bone quality and body mass index on periprosthetic femoral fractures: a biomechanical laboratory study. Med. Sci. Monit. Int. Med. J. Exp. Clin. Res. 15 (11), BR307–312.

Jasty, M., Henshaw, R.M., O'Connor, D.O., Harris, D.H., Oct. 1993. High assembly strains and femoral fractures produced during insertion of uncemented femoral components. J. Arthroplast. 8 (5), 479–487. https://doi.org/10.1016/S0883-5403(06)80213-5.

Johnson, A.J., Desai, S., Zhang, C., Koh, K., Zhang, L.-Q., Costales, T., O'Toole, R.V., Manson, T.T., Aug. 2020. A calcar collar is protective against early torsional/spiral periprosthetic femoral fracture: a paired cadaveric biomechanical analysis. J. Bone Joint Surg. 102 (16), 1427–1433. https://doi.org/10.2106/JBJS.19.01125.

Kistler, M., Steinbrück, A., Schmidutz, F., Paulus, A.C., Holzapfel, B.M., Woiczinski, M., May 2024. The effect of a collar on primary stability of standard and undersized cementless hip stems: a biomechanical study. Arch. Orthop. Trauma Surg. https://doi.org/10.1007/s00402-024-05374-7.

Konow, T., Baetz, J., Melsheimer, O., Grimberg, A., Morlock, M., Apr. 2021. Factors influencing periprosthetic femoral fracture risk: a German registry study. Bone Joint J. 103-B (4), 650–658. https://doi.org/10.1302/0301-620X.103B4.BJJ-2020-1046.R2.

Konow, T., Schlieker, P.J., Lampe, F., Ondruschka, B., Morlock, M.M., Huber, G., Nov. 2022. Influence of bone morphology and femur preparation method on the primary stability of hip revision stems. J. Orthop. Res., jor.25481 https://doi.org/10.1002/jor.25481.

Lamb, J.N., Baetz, J., Messer-Hannemann, P., Adekanmbi, I., van Duren, B.H., Redmond, A., West, R.M., Morlock, M.M., Pandit, H.G., Jul. 2019. A calcar collar is

protective against early periprosthetic femoral fracture around cementless femoral components in primary total hip arthroplasty: a registry study with biomechanical validation. Bone Joint J. 101-B (7), 779–786. https://doi.org/10.1302/0301-620X.101B7.BJJ-2018-1422.R1.

Lamb, J.N., Evans, J.T., Relton, S., Whitehouse, M.R., Wilkinson, J.M., Pandit, H., Oct. 2024. The incidence of postoperative periprosthetic femoral fracture following total hip replacement: an analysis of UK national joint registry and hospital episodes statistics data. PLoS Med. 21 (10), e1004462. https://doi.org/10.1371/journal.pmed.1004462.

Levadnyi, I., Gubaua, J.E., Dicati, G.W.O., Awrejcewicz, J., Gu, Y., Pereira, J.T., Loskutov, A., Dec. 2021. Comparative analysis of the biomechanical behavior of collar and collarless stems: experimental testing and finite element modelling. J. Med. Biol. Eng. 41 (6), 844–855. https://doi.org/10.1007/s40846-021-00652-w.

Magill, P., Blaney, J., Hill, J.C., Bonnin, M.P., Beverland, D.E., Dec. 2016. Impact of a learning curve on the survivorship of 4802 cementless total hip arthroplasties. Bone Joint J. 98-B (12), 1589–1596. https://doi.org/10.1302/0301-620X.98B12.BJJ-2016-0203.R1.

Mansour, H.A., Ray, J.D., Mukherjee, D.P., 1995. Stress shielding of femoral component with and without collar. In: Proceedings of the 1995 Fourteenth Southern Biomedical Engineering Conference. IEEE, Shreveport, LA, USA, pp. 53–54. https://doi.org/10.1109/SBEC.1995.514429.

McConnell, J.S., Syed, F.A., Saunders, P., Kattimani, R., Ugwuoke, A., Magra, M., Young, S.K., Mar. 2021. Definition and validation of a system for classifying the undersized Corail femoral stem in total hip arthroplasty. Hip Int., 112070002199600 https://doi.org/10.1177/1120700021996001.

Meding, J.B., Ritter, M.A., Keating, E.M., Faris, P.M., Apr. 1997. Comparison of collared and collarless femoral components in primary uncemented total hip arthroplasty. J. Arthroplast. 12 (3), 273–280. https://doi.org/10.1016/S0883-5403(97)90023-1.

Melbye, S.M., Haug, S.C.D., Fenstad, A.M., Furnes, O., Gjertsen, J.-E., Hallan, G., Oct. 2021. How does implant survivorship vary with different Corail femoral stem variants? Results of 51,212 cases with up to 30 years of follow-up from the Norwegian arthroplasty register. Clin. Orthop. 479 (10), 2169–2180. https://doi.org/10.1097/CORR.0000000000001940.

Milgrom, C., Simkin, A., Eldad, A., Nyska, M., Finestone, A., Mar. 2000. Using bone's adaptation ability to lower the incidence of stress fractures. Am. J. Sports Med. 28 (2), 245–251. https://doi.org/10.1177/03635465000280021701.

Mont, M., Maar, D., Krackow, K., Hungerford, D., Mar. 1992. Hoop-stress fractures of the proximal femur during hip arthroplasty. Management and results in 19 cases. J. Bone Joint Surg. (Br.) 74-B (2), 257–260. https://doi.org/10.1302/0301-620X.74B2.1544964.

Morlock, M., Perka, C., Melsheimer, O., Kirschbaum, S.M., Mar. 2024. Influence of the type of stem and its fixation on revision and immediate postoperative mortality in elective total hip arthroplasty. Bone Joint J. 106-B (3 Supple A), 130–136. https://doi.org/10.1302/0301-620X.106B3.BJJ-2023-0820.R2.

Park, C.-W., Lim, S.-J., Ye, D.-H., Park, Y.-S., Oct. 2020. Outcomes of cerclage cabling for intraoperative calcar cracks in cementless total hip arthroplasty using broach-only, tapered wedge stems. J. Arthroplast. 35 (10), 3002–3009. https://doi.org/10.1016/j.arth.2020.05.041.

Püschel, K., Heinemann, A., Dietz, E., Hellwinkel, O., Henners, D., Fitzek, A., Dec. 2020. New developments and possibilities in the field of post-mortem medicine mortui vivos docent. Rechtsmedizin 30 (6), 425–429. https://doi.org/10.1007/s00194-020-00402-3.

Reilly, D.T., Burstein, A.H., Jan. 1975. The elastic and ultimate properties of compact bone tissue. J. Biomech. 8 (6), 393–405. https://doi.org/10.1016/0021-9290(75)90075-5.

Rosemont, I., 2024. American Joint Replacement Registry (AJRR): 2024 Annual Report. American Academy of Orthopaedic Surgeons (AAOS). Accessed: May 04, 2025. [Online]. Available: https://connect.registryapps.net/hubfs/AJRR/AJRR%202024%20Annual%20Report.pdf.

Rudman, K., Aspden, R., Meakin, J., Dec. 2006. Compression or tension? The stress distribution in the proximal femur. Biomed. Eng. Online 5 (1), 12. https://doi.org/10.1186/1475-925X-5-12.

Schwartz Jr., J.T., Mayer, J.G., Engh, C.A., Sep. 1989. Femoral fracture during non-cemented total hip arthroplasty. J. Bone Joint Surg. Am. 71 (8), 1135–1142.

Simpson, D.J., Kendrick, B.J.L., Hughes, M., Glyn-Jones, S., Gill, H.S., Rushforth, G.F., Murray, D.W., Oct. 2010. The migration patterns of two versions of the furlong cementless femoral stem: a randomised, controlled trial using radiostereometric analysis. J. Bone Joint Surg. (Br.) 92-B (10), 1356–1362. https://doi.org/10.1302/0301-620X.92B10.24399.

Syed, F., Hussein, A., Katam, K., Saunders, P., Young, S.K., Faisal, M., Nov. 2018. Risk of subsidence and peri-prosthetic fractures using collared hydroxyapatite-coated stem for hip arthroplasty in the elderly. Hip Int. 28 (6), 663–667. https://doi.org/10.1177/1120700017754085.

Varga, P., Schwiedrzik, J., Zysset, P.K., Fliri-Hofmann, L., Widmer, D., Gueorguiev, B., Blauth, M., Windolf, M., Apr. 2016. Nonlinear quasi-static finite element simulations predict in vitro strength of human proximal femora assessed in a dynamic sideways fall setup. J. Mech. Behav. Biomed. Mater. 57, 116–127. https://doi.org/10.1016/j.jmbbm.2015.11.026.

Waligora, A.C., Owen, J.R., Wayne, J.S., Hess, S.R., Golladay, G.J., Jiranek, W.A., Jun. 2017. The effect of prophylactic cerclage wires in primary total hip arthroplasty: a biomechanical study. J. Arthroplast. 32 (6), 2023–2027. https://doi.org/10.1016/j.arth.2017.01.019.

Weightman, B., Freeman, M., Revell, P., Braden, M., Albrektsson, B., Carlson, L., Aug. 1987. The mechanical properties of cement and loosening of the femoral component of hip replacements. J. Bone Joint Surg. (Br.) 69-B (4), 558–564. https://doi.org/10.1302/0301-620X.69B4.3611159.

Wendler, T., Fischer, B., Brand, A., Weidling, M., Fakler, J., Zajonz, D., Osterhoff, G., Dec. 2022. Biomechanical testing of different fixation techniques for intraoperative proximal femur fractures: a technical note. Int. Biomech. 9 (1), 27–32. https://doi.org/10.1080/23335432.2022.2142159.